



Published in final edited form as:

*Oncogene*. 2014 May 15; 33(20): 2589–2600. doi:10.1038/onc.2013.226.

## Downregulation of miR-140 promotes cancer stem cell formation in basal-like early stage breast cancer

Q Li, Y Yao, G Eades, Z Liu, Y Zhang, and Q Zhou

Greenebaum Cancer Center, Department of Biochemistry and Molecular Biology, University of Maryland School of Medicine, Baltimore, MD, USA

### Abstract

The major goal of breast cancer prevention is to reduce the incidence of ductal carcinoma *in situ* (DCIS), an early stage of breast cancer. However, the biology behind DCIS formation is not well understood. It is suspected that cancer stem cells (CSCs) are already programmed in pre-malignant DCIS lesions and that these tumor-initiating cells may determine the phenotype of DCIS.

MicroRNA (miRNA) profiling of paired DCIS tumors revealed that loss of miR-140 is a hallmark of DCIS lesions. Previously, we have found that miR-140 regulates CSCs in luminal subtype invasive ductal carcinoma. Here, we find that miR-140 has a critical role in regulating stem cell signaling in normal breast epithelium and in DCIS. miRNA profiling of normal mammary stem cells and cancer stem-like cells from DCIS tumors revealed that miR-140 is significantly downregulated in cancer stem-like cells compared with normal stem cells, linking miR-140 and dysregulated stem cell circuitry. Furthermore, we found that SOX9 and ALDH1, the most significantly activated stem-cell factors in DCIS stem-like cells, are direct targets of miR-140. Currently, targeted therapies (tamoxifen) are only able to reduce DCIS risk in patients with estrogen receptor  $\alpha$  (ER $\alpha$ )-positive disease. We examined a model of ER $\alpha$ -negative/basal-like DCIS and found that restoration of miR-140 via a genetic approach or with the dietary compound sulforaphane decreased SOX9 and ALDH1, and reduced tumor growth *in vivo*. These results support that a miR-140/ALDH1/SOX9 axis is critical to basal CSC self-renewal and tumor formation *in vivo*, suggesting that the miR-140 pathway may be a promising target for preventative strategies in patients with basal-like DCIS.

### Keywords

microRNAs; ductal carcinoma *in situ*; cancer stem cells; basal-like breast cancer

## INTRODUCTION

Ductal carcinoma *in situ* (DCIS) is a noninvasive early breast cancer, totally confined to the mammary duct.<sup>1</sup> DCIS currently accounts for 25% of new breast cancer cases in the United

© 2013 Macmillan Publishers Limited All rights reserved

Correspondence: Dr Q Zhou, Greenebaum Cancer Center, Department of Biochemistry and Molecular Biology, University of Maryland School of Medicine, 108 North Greene Street, RM 337, Baltimore, MD 21201, USA., qzhou@som.umaryland.edu.

### CONFLICT OF INTEREST

The authors declare no conflict of interest.

States.<sup>2</sup> Prior to widespread mammography, DCIS detection was rare.<sup>3</sup> Most DCIS is detected by mammography as clustered microcalcifications.<sup>4</sup> DCIS is classified by nuclear grade (low, intermediate and high), the presence of necrosis<sup>1,5</sup> and genetic markers (for example, ER or HER2 status). Left untreated, DCIS may progress to invasive disease, with higher grade DCIS demonstrating greater risk of progression.<sup>5,6</sup> Lumpectomy followed by radiation therapy is the standard of care for DCIS.<sup>7</sup> Following treatment, ~15% of patients show recurrent disease.<sup>8</sup>

Like invasive tumors, DCIS are heterogeneous lesions with differing malignant potential.<sup>9</sup> The underlying biology of DCIS is poorly understood and clinicians cannot predict recurrence or invasive progression. Adjuvant tamoxifen treatment is administered to decrease the risk of disease recurrence, however, this is only beneficial to patients with estrogen receptor  $\alpha$  (ER $\alpha$ )-positive DCIS, whereas basal-like DCIS remains a therapeutic challenge.<sup>10,11</sup>

Studies suggest that malignant precursor cells exist in DCIS lesions.<sup>12</sup> Cancer stem cells (CSCs) are suspected to have important roles in tumor formation, drug resistance and disease recurrence.<sup>13,14</sup> It has recently been shown that DCIS tumors may contain a population of self-renewing CSCs.<sup>15</sup> It is possible that DCIS CSCs may predetermine the malignant potential of DCIS lesions.

MicroRNAs (miRNAs) are dysregulated in nearly every type of human cancer.<sup>16</sup> For breast tumors, miRNAs regulate nearly every hallmark of tumorigenesis.<sup>17</sup> Epigenetic mechanisms are important in controlling tissue-specific miRNA expression, in particular, DNA and histone methylation have critical roles in regulating miRNA expression during mammaryogenesis.<sup>18</sup> Not surprisingly, epigenetic mechanisms are frequently implicated in miRNA dysregulation in breast tumors.

Genome-wide miRNA profiling has uncovered unique miRNA expression within DCIS lesions.<sup>19</sup> Deep sequencing technology identified 66 miRNAs that were dysregulated in DCIS, compared with normal tissues.<sup>20</sup> Among the few DCIS profiles that exist, there is large variation and little consensus due to tumor heterogeneity and normal tissue selection. In the present study, we conducted miRNA profiling analyses among different subtypes of DCIS lesions and found that miR-140 is reproducibly altered in DCIS and invasive ductal carcinoma, both here and in previous studies.<sup>20</sup> However, the functional attributes of this miRNA signature in DCIS lesions have not been examined. We delineate subtype-specific miR-140 loss that may selectively contribute to the growth and survival of CSCs in basal-like DCIS lesions.

## RESULTS

### miRNA profiling from DCIS lesions and matched normal breast tissues

To identify miRNAs that are significantly altered within DCIS lesions, we performed genome-wide microarray analysis comparing miRNA expression in DCIS tumors to matched normal tissue controls (Supplementary Figure S1A). We chose DCIS samples covering both ER $\alpha$ -positive and -negative tumors from a wide range of ages and race. In our

array studies, 68 miRNAs were significantly dysregulated ( $P < 0.05$ ) in DCIS tissue compared with controls. We examined these 68 dysregulated miRNAs by tumor grade in side-by-side comparisons (Figure 1). Next, we compared our results to those from published studies.<sup>20</sup> Our criteria for follow-up analysis included miRNAs that were (1) among the most consistent markers of DCIS from independent studies, (2) were known to target stem cell self-renewal regulators or (3) those miRNAs previously implicated in invasive breast cancer. One of the most reproducible miRNA signatures we identified was miR-140 downregulation, which was consistent across independent profiles of DCIS lesions. We found that expression of miR-140 in low-grade DCIS most resembled normal tissue. Furthermore, we found that miR-140 showed progressive downregulation along increasing DCIS grade, showing the greatest alterations in the high-grade DCIS. Based on analysis of our results and those of others, we reasoned that this previously uncharacterized miRNA, miR-140, should be selected for subsequent analysis, as it represents a potential tumor suppressor in DCIS lesions.

### Validation of miR-140 downregulation in different breast cancer tissues

To confirm our microarray data, we subjected miR-140 to subsequent validation in additional patient samples. We examined 22 frozen DCIS tumors of various histological grades (grade I,  $n = 7$ ; grade II,  $n = 7$ ; grade III,  $n = 8$ ) for miR-140 expression by quantitative real-time polymerase chain reaction (qRT-PCR). We observed miR-140 loss in all the 22 DCIS samples (Figure 2a results representative of basal-like samples). These results indicate that miR-140 loss is a common event in DCIS development.

Next, we used *in situ* hybridization staining of miR-140 to visualize expression in paraffin-embedded breast tissues. We used miR-140 RNA probes labeled with 5'-digoxigenin. This approach allows us to detect miR-140 levels within mammary epithelial cells in the context of mammary architecture. We examined miR-140 across a broad selection of breast tumor tissues to determine whether miR-140 was specific to DCIS. As shown in Figure 2b, we found miR-140 downregulation across every type of breast malignancy. These results confirmed miR-140 loss within DCIS cancer cells.

### Epigenetic dysregulation of miR-140 in DCIS lesions

After successful validation of our microarray results, we next turned our attention to examine the molecular mechanisms underlying miR-140 downregulation in DCIS. Studies from ours and other laboratories have shown that miRNA expression in mammary epithelium is frequently regulated epigenetically.<sup>21–23</sup> For this reason, we tested whether miRNA dysregulation in DCIS involves epigenetic reprogramming. miR-140 is a miRtron encoded with an intronic region of *WWP2*, an E3 ubiquitin ligase.<sup>24</sup> We examined DNA methylation of the *WWP2*/miR-140 locus. Using the CpG Island Searcher tool<sup>25</sup> we identified two CpG Islands within the *WWP2* locus (Figure 3a). Using bisulfite sequencing we examined CpG methylation status of these predicted CpG islands in breast cancer cell lines and tumor tissues.

Basal-like DCIS is aggressive, at a high risk for invasion, is poorly differentiated and is without molecularly targeted therapies.<sup>10,26,27</sup> Based on these challenges we chose

MCF10DCIS, a model cell line of poorly differentiated basal-like DCIS (lacking ER $\alpha$  expression) for further study.<sup>28–30</sup> When injected into the mammary glands of nude mice, MCF10DCIS forms well recognizable DCIS lesions.<sup>28</sup> MCF10DCIS cells were derived from MCF-10A nontumorigenic mammary epithelial cells and demonstrate significant loss of miR-140 expression compared with parental MCF-10A cells (Supplementary Figure S1B).

We found that CpG Island 1 was always unmethylated in normal breast tissues and in breast tumors. However, CpG Island 2 was found to be differentially methylated between normal tissues and breast tumors. Fifty percent of the CpGs were methylated in CpG Island 2 in nontumorigenic MCF-10A cells. Similar methylation levels were detected in other normal mammary epithelial cell lines (HME, ERIN) and in primary human mammary epithelial cells. However, in MCF10DCIS cells, 69.8% of the CpGs were methylated, roughly a 20% increase. Similar results were observed in basal-like atypical ductal hyperplasia, DCIS and invasive ductal carcinoma tumor tissues ( $n = 4$ , data not shown). To establish a link between this differential CpG methylation and changes in miR-140 expression, we treated MCF10DCIS cells with epigenetic therapy, either 5-aza-2-deoxycytidine (a DNA methyltransferase inhibitor) or sulforaphane (demonstrates dual inhibition of histone deacetylase activity and DNA methyltransferase expression<sup>31,32</sup>). We found that epigenetic therapy was able to restore normal methylation levels in MCF10DCIS cells and activate miR-140 expression (Figures 3b and c).

### miR-140 is a tumor suppressor in a model of basal-like DCIS

Next, we investigated the potential biological impact of miR-140 loss on the tumorigenic properties of DCIS and invasive breast cancer cell lines. We tested the impact of miR-140 overexpression in MCF10DCIS cells on anchorage-independent growth in soft agar. miR-140 overexpression resulted in a statistically significant decrease in soft agar colony formation in MCF10DCIS cells. We also included MCF-7 cells (invasive luminal breast cancer) as a positive ‘transformed’ control for anchorage-independent growth (Figures 4a and b; Supplementary Figure S2). These findings support a tumor-suppressive role of miR-140 in DCIS.

Next, we explored the phenotype of miR-140 loss in normal mammary epithelial cells using three-dimensional (3D) cell culture. 3D cell culture can be used to recapitulate mammary organogenesis *in vitro*. It has been previously shown that only mammary progenitors or mammary stem cells can grow in 3D cell culture.<sup>33,34</sup> 3D cell culture can be used to investigate the process of cellular differentiation, and to study the multicellular architecture of the mammary gland. We investigated the impact of miR-140 knockdown and miR-140 overexpression on MCF-10A mammary epithelial cells in 3D cell culture. As shown in Figures 4c and d, we found that miR-140 knockdown resulted in increased proliferation as evidenced by staining for proliferative marker Ki67, whereas miR-140 overexpression resulted in decreased proliferation (decreased Ki67). An important step in acini formation in 3D cell culture involves luminal formation via programmed cell death, ‘hollowing’ of the lumen. We examined this phenomenon by staining for active Caspase-3 expression. Knockdown of miR-140 resulted in decreased rates of luminal apoptosis, as evidenced by

decreased activated-Caspase-3 staining (Figure 5a). Overexpression of miR-140 resulted in increased active Caspase-3 staining, indicating an increase in luminal apoptosis. These results indicate that the growth and maintenance of the mammary tree can be modified through the manipulation of miR-140 levels.

### miR-140 downregulation in DCIS stem cells

As miR-140 modulation was found to have an impact on acini formation, and as only mammary progenitors or mammary stem cells can form organoid or acini structure in Matrigel (Figures 4 and 5), these findings suggested that miR-140 might be a stem cell regulator in breast tissue. We investigated what role miR-140 may have in regulating normal mammary epithelial stem cells and DCIS stem-like cells. First, we performed a comparison of miRNA expression in normal cells versus cancer stem-like cells. We separated normal and breast CSCs using fluorescent-activated cell sorting for CD44 high/CD24 low populations of cells, subpopulations previously associated with stemness in breast tumors and normal breast tissues.<sup>35,36</sup> Previously, basal-like invasive breast cancers were found to possess higher levels of CD44 high/CD24 low cells.<sup>37,38</sup> It was also shown that ALDH1 activity was highest in the basal-like breast cancer subtype.<sup>37,38</sup> We found high levels of ALDH1 expression in our isolated CD44 high/CD24 low MCF10DCIS cells, indicating that our DCIS model contains a subpopulation of cancer cells with stem-like properties. We next performed microarray analysis on these CSCs. As shown in Figure 6a, 72 miRNAs were found to be differentially expressed between normal mammary epithelial stem cells isolated from MCF-10A cells and stem-like cells isolated from MCF10DCIS cells. miR-140 was among the most significantly downregulated miRNA in cancer stem-like cells, down – 13.55-fold compared with its (already low) expression in mammary stem cells. These findings strongly suggest that the role of miR-140 in DCIS may be related to dysregulated stem cell signaling and the emergence or maintenance of DCIS CSCs.

### SOX9 and ALDH1 stem cell regulators are critical targets of miR-140 in DCIS stem cells

We next wanted to identify which pathways were regulated by miR-140 in DCIS stem-like cells. We began by investigating breast cancer-related targets of miR-140 using the TargetScan bioinformatic prediction algorithm. Among the predicted targets of miR-140 are numerous mRNAs associated with embryonic (SOX2, KLF4), adult (NOTCH2, WNT4) or neoplastic (ALDH1, IL6R and ABCA1/10) stem cells. We constructed miR-140 expression constructs and stably transfected MCF-10A cells using lentiviral infection. We collected mRNA from pooled cell populations and then attempted the validation of these numerous miR-140-related targets. Using qRT-PCR we examined the expression of these mRNAs following miR-140 overexpression (Figure 5b), finding that many of these stem cell-related targets are regulated by miR-140 in mammary epithelial cells. These results suggest that miR-140 involvement in DCIS may indeed be related to its regulation of stem cell circuitry.

Since we found that overexpression of miR-140 resulted in the targeting of numerous stem cell signaling pathways in mammary epithelial cells, we further investigated if loss of regulation of any of these pathways may contribute to CSC growth or maintenance in DCIS. As we were particularly interested in which pathways contribute to the malignant properties of CSCs compared with tightly regulated normal stem cells, we compared expression of

several of these genes in MCF10DCIS stem-like cancer cells to stem cells isolated from parental MCF-10A cells. Among these miR-140 targets, we found that SOX9, a transcription factor previously associated with miR-140 expression<sup>24</sup> and recently shown to be a master regulator of mammary stem cell state,<sup>39</sup> and ALDH1, an enzyme that oxidizes aldehydes and is a marker of breast CSCs and poor prognosis,<sup>40</sup> were both dramatically upregulated in MCF10DCIS stem-like cells compared with MCF-10A normal mammary stem cells (Figure 6b upper panel; Supplementary Figure S2). Furthermore, forced miR-140 expression did not result in dramatic downregulation of other prospective mRNA targets in DCIS stem-like cells (Figure 6b lower panel, representative data shown), suggesting that miR-140 may regulate specific pathways in DCIS CSCs. Furthermore, these results suggest a potential mechanism behind CSC emergence in DCIS cells, miR-140 downregulation resulting in overexpression of SOX9 and ALDH1, potentially representing loss of regulation or hijacking of stemness circuitry from mammary stem cells.

To validate miR-140 targeting of SOX9 mRNA and ALDH1 mRNA 3'-untranslated regions (UTRs), we cloned the SOX9 and ALDH1 3'-UTRs into luciferase constructs based on the location of predicted miRNA response elements (Figures 6c and d). Overexpression of miR-140 reduced the luciferase activity of SOX9 3'-UTR and ALDH1 3'-UTR reporter constructs in 293T cells. Mutation of the miR-140 miRNA response elements in the SOX9 3'-UTR and ALDH1 3'-UTR effectively blocked miR-140 targeting, resulting in restored luciferase activity and demonstrating specificity of miR-140 interactions with the predicted targeting sites in the SOX9 and ALDH1 3'-UTRs. We examined the impact of forced miR-140 expression on SOX9 and ALDH1 protein levels in MCF10DCIS cells and in SUM102PT cells, a basal-like cancer cell line derived from a patient with apocrine invasive ductal carcinoma and high levels of DCIS.<sup>41</sup> We found that miR-140 overexpression resulted in downregulation of SOX9 and ALDH1 protein levels in both cell lines (Supplementary Figure S3).

### **SOX9 is overexpressed in multiple breast cancer malignancies, including DCIS**

Previous research has shown that SOX9 is a master regulator for mammary stemness.<sup>39</sup> Having found a link between miR-140 and SOX9 regulation, we wanted to further investigate the role of SOX9 in breast malignancies. Using western blotting we found that SOX9 was overexpressed in MCF10DCIS cells compared with nontumorigenic MCF-10A mammary epithelial cells (Figure 7a). Next, we examined SOX9 expression across a tissue array of multiple types of breast tumor tissues using immunohistochemistry. We found that SOX9 was significantly overexpressed in tumor tissues from multiple breast malignancies (Figures 7b and c). Interestingly, SOX9 shows progressively increased staining from low- to high-grade DCIS corresponding with a progressive loss of miR-140 (Figure 1a).

### **The miR-140/SOX9 pathway critically regulates mammosphere formation in mammary stem cells and DCIS stem cells**

Having demonstrated a link between miR-140 and regulation of stem-cell factors in DCIS cells, we next examined the functional impact of miR-140 modulation of DCIS stem-like cells *in vitro*. Mammosphere formation is a surrogate for mammary stem cell and breast CSC growth and expansion.<sup>42</sup> We examined miR-140 overexpression and knockdown on

mammosphere formation in MCF-10A mammary epithelial cells. MiR-140 overexpression resulted in smaller and fewer mammospheres (Figures 7d and e), whereas miR-140 knockdown resulted in increased mammosphere formation (Supplementary Figure S4). In MCF10DCIS cells, which express low levels of miR-140, re-expression of miR-140 resulted in a significant decrease in mammosphere formation (Figures 7f and g).

In normal mammary tissue, low levels of SOX9 correlate with tightly controlled mammary gland growth and differentiation. Mammary stem cells were found to express SOX9, whereas differentiated mammary cells express low levels of SOX9. It was shown that SOX9 is a critical mammary stem cell regulator.<sup>39</sup> We found that SOX9 was undetectable by western blot in MCF-10A cells, whereas MCF10DCIS cells demonstrated significant SOX9 overexpression (Figure 7a). We next tested the effect of SOX9 modulation on mammosphere formation. SOX9 knockdown resulted in decreased mammosphere formation in MCF10DCIS cells, whereas SOX9 overexpression resulted in a significant increase in sphere formation in MCF-10A cells (Figures 7d–g). This indicates that SOX9 is an important stem cell regulator in our model, and that transformation is associated with the disturbance of these normal stem cell pathways.

Together, these results offer support for the hypothesis that miR-140 loss and subsequent SOX9 overexpression result in dysregulated stem cell signaling in DCIS CSCs. Furthermore, we demonstrate that using genetic tools to activate miR-140 or target aberrant SOX9 signaling can partially restore normal stem cell regulation *in vitro*.

### Activation of miR-140 reduces stem cell renewal and tumor growth *in vivo*

We next set out to test our results from cell culture models regarding miR-140 and DCIS cancer stem-like cells *in vivo*. 10<sup>6</sup> MCF10DCIS cells overexpressing control vector or miR-140 expression vector in a 1:1 mixture of media and Matrigel were transplanted into mammary glands of nude mice. Tumor volume was measured weekly. We found that miR-140-overexpressing DCIS cells demonstrated significantly decreased tumor growth in nude mice (Figure 8a).

The defining feature of CSCs is the enhanced xenograft-initiation capacity.<sup>13</sup> To verify that miR-140 overexpression reduced the xenograft-initiating capacity of DCIS stem-like cells, we performed similar xenograft experiments, except this time we transplanted a limiting number (10 000 cells) of mammosphere-cultured cells (enriched in DCIS CSCs). Mammosphere cells resulted in much faster growing tumors than whole-cell populations, demonstrating the high tumorigenicity expected from these CSC-enriched cells (Figure 8b). Altogether 10 000 cells from whole-cell populations failed to result in any tumors, 10 000 control mammosphere cells resulted in tumors that by 4 weeks surpassed 200 mm<sup>3</sup>, whereas whole-cell population control tumors (10<sup>6</sup> cells) just surpassed 100 mm<sup>3</sup>. We found that miR-140 overexpression nearly eliminated growth of DCIS tumors from mammosphere cells.

Finally, we examined tumor growth of purified MCF10DCIS stem-like cells (CD44 high/CD24 low). Injection of only 6000 DCIS stem-like cells resulted in fast-growing tumors that by 4 weeks reached 400 mm<sup>3</sup> volume. As we had previously shown that miR-140 could be

activated by epigenetic therapy *in vitro*, we wanted to examine whether epigenetic treatment could lead to re-expression of miR-140 and subsequently inhibit DCIS growth *in vivo*. It is well known that epigenetic drugs have been shown to be able to specifically target CSCs for elimination.<sup>43</sup> However, many epigenetic drugs show high levels of toxicity *in vivo*. Fortunately, some well-tolerated dietary compounds have been shown to be powerful epigenetic activators including the isothiocyanate sulforaphane.<sup>31</sup> We found that sulforaphane treatment of MCF10DCIS stem-like cells significantly inhibited tumor growth (Figure 8c). Furthermore, in isolated tumor cells we found that sulforaphane treatment resulted in upregulation of miR-140, and downregulation of SOX9 and ALDH1 *in vivo* (Figure 8d). Taken together, these results support that miR-140 regulates DCIS tumor formation *in vivo* and that miR-140-targeted therapy might be an effective therapeutic approach for DCIS prevention.

Finally, we also examined MDA-MB-231 cells, a model of triple negative, basal-like invasive breast cancer to confirm our results in an additional breast cancer xenograft model. We found that miR-140 levels were very low in MDA-MB-231 cells compared with normal mammary epithelial cells (HME) (Supplementary Figure S5A). Furthermore, treatment with the epigenetic modulator sulforaphane resulted in miR-140 upregulation and decreased stem-like cell frequency (as defined by CD44 high/CD24 low) in MDA-MB-231 cells (Supplementary Figures S5A and S5B). Finally, we examined the effect of sulforaphane treatment on tumor xenografts of MDA-MB-231 cancer stem-like cells. Sulforaphane treatment resulted in decreased tumor growth (Supplementary Figure S5C). These results provide additional support regarding the importance of miR-140 regulation of breast CSCs in basal-like breast tumors.

## DISCUSSION

Previous studies have shown that miRNAs can regulate both mammary stem cells and breast CSCs.<sup>36</sup> For example, miR-200 has been previously found to regulate both normal and neoplastic breast stem cells.<sup>36,44</sup> When comparing miRNA expression of mammary stem cells and DCIS stem cells, miR-140 was among the most significantly downregulated miRNAs. This indicates that miR-140 may regulate tightly controlled mammary stem cell circuitry, and that miR-140 dysregulation may contribute to DCIS CSC formation.

It is likely that miR-140 has stage-specific and subtype-specific roles in breast tumors. As with all miRNAs, the impact of miR-140 dysregulation is dependent on its cumulative effects, and depends on the types of targets present in a given tissue or tumor. We attempted to identify the most critical stem cell-related targets of miR-140 by examining only targets that were dysregulated in DCIS stem cells compared with normal mammary stem cells. We found that SOX9 and ALDH1 were significantly dysregulated in DCIS stem-like cells and we confirmed that both are direct targets of miR-140 regulation in DCIS stem-like cells. Recently, Weinberg and colleagues<sup>39</sup> has shown that differentiated mammary epithelial cells can be reprogrammed to multipotent mammary stem cells through forced expression of stem cell transcription factors. One part of mammary reprogramming involved an epithelial to mesenchymal transition (EMT) step (introduction of Slug) and the other involved forced expression of a master regulator of mammary stemness, SOX9. Discovering that miR-140



can directly target SOX9 in DCIS stem cells suggests that miR-140 loss can subvert an absolutely critical regulator of breast tissue differentiation potential, which might lead to *de novo* CSC formation by hijacking mammary stem cell transcriptional programs.

Our profiling of DCIS stem-like cells also revealed downregulation of miR-200 family (regulators of EMT and polycomb<sup>36,44</sup>), let-7 (regulators of Ras and polycomb<sup>45,46</sup>) and miR-30a (regulator of Snail1<sup>47</sup>), suggesting that EMT-like transformation, embryonic epigenetic programs and mammary stem cell circuitry are all also activated in DCIS stem cells.

Finally, we were able to show *in vivo* that miR-140 activation through genetic approaches or epigenetic drugs reduced the tumorigenic potential of DCIS stem-like cells. The primary goal of breast cancer chemoprevention is preventing DCIS formation. Taken together, our results suggest that DCIS CSCs and, more specifically, loss of miRNA regulation of stem cell circuitry may contribute to DCIS formation.

Targeting DCIS CSCs may eliminate the malignant/invasive component of DCIS lesions and prevent recurrence or disease progression.<sup>12</sup> Our results suggest a potential targetable pathway for eliminating DCIS, the miR-140/SOX9 pathway. As the only currently available preventative therapy used in treating patients with DCIS is tamoxifen, our findings suggest potential chemoprevention targets and therapeutic strategies for patients with ER $\alpha$ -negative disease, the miR-140/SOX9 pathway.

## MATERIALS AND METHODS

### Cell culture

MCF10DCIS, SUM225CWN, SUM102PT were grown in Dulbecco's modified Eagle medium/F-12 +5% horse serum (Invitrogen, Carlsbad, CA, USA) and 1% L-Glut. MCF-10A were grown in Dulbecco's modified Eagle medium/F-12 medium supplemented with 10  $\mu$ g/ml insulin, 100 ng/ml cholera toxin, 0.5  $\mu$ g/ml hydrocortisone (Sigma, St Louis, MO, USA), 20 ng/ml EGF and 5% horse serum (Invitrogen). Cells were incubated in 5% CO<sub>2</sub> at 37 °C.

### Quantitative real-time PCR

qRT-PCR analysis of mRNA/miRNA expression was performed as previously described with normalization to GAPDH mRNA or U6 small nuclear RNA.<sup>21</sup> Primer sequences are listed in the supplemental materials.

### Immunohistochemistry and western blotting

Immunostaining of paraffin-embedded breast tumor tissues was performed as previously described<sup>21</sup> using polyclonal rabbit anti-sox9 antibody (Santa Cruz Biotechnology, Inc., Santa Cruz, CA, USA). Western blotting was performed as previously described<sup>21</sup> using SOX2 (Neuromics, Edina, MN, USA), SOX9 (Millipore, Billerica, MA, USA),  $\beta$ -Actin (Sigma) and ALDH1 (BD Pharmingen, San Diego, CA, USA) antibodies.

### Mammosphere assay

Cells were separated using cell dissociation buffer (Millipore) and 40- $\mu$ m strainers (Fisher Scientific, Pittsburgh, PA, USA). A total of 20 000 cells/ml were seeded in six-well plates coated with 2% polyhema (Sigma). After 7 days, spheres >100  $\mu$ m were quantified.

### Transfections and luciferase assays

Cells were infected with miR-140 expression vector, SOX9 expression vector or control vectors using lentiviral infection as previously described.<sup>21</sup> Dual luciferase assays were performed as previously described.<sup>21</sup>

The 3'-UTR of ALDH1A3 and SOX9 was amplified by PCR and cloned into *NheI* and *XhoI* sites of pSGG vector. Control reporter plasmids were used to generate a mutant miRNA response element for miR-140-3p using the Generate site-directed mutagenesis system (Invitrogen). The resulting ALDH1A3 mutant contains three point mutations CCCC(T-to-A)G (T-to-A)G(G-to-C)TGT GGTTC, and the SOX9 mutant contains two point mutations GATCAGC(C-to-G)C(A-to-T)CTGACA, as confirmed by sequencing.

### Bisulfite mapping

A genomic DNA segment (Chromosome 16: 68350775–68533144) encompassing *WWP2* gene (NM\_007014.3) and upstream sequence (3 kb) was analyzed with CpG Island searcher software (<http://cpgislands.usc.edu/cpg.aspx>). Bisulfite sequencing was performed as previously described<sup>21</sup> using wwp2L (5'-GTTTTTTGTGGGAGGGGTTT-3') and wwp2R (5'-CTAAAAA CCTAAACTCCTCTCCCTTC-3') primers.

### Microarray

A total of 200 ng total RNA from fresh tumor tissues was hybridized to GeneChip miRNA Array v3.0 (Affymetrix, Santa Clara, CA, USA). Flow cytometry was performed on cells co-stained with CD44-APC and CD24-PE antibodies (BD Pharmingen). Total RNA was isolated from stem cells (CD44 high/CD24 low) using miRNeasy Mini Kit (Qiagen, Valencia, CA, USA). Hybridization and measurements were performed by the University of Maryland Biopolymer-Genomics Core. We normalized and preprocessed gene expression with quantile normalization, and identified top miRNAs based on both statistical significance (Student's *t*-test,  $P < 0.05$ ) and more than two-fold expression changes. Heatmap and hierarchical clusters for selected miRNAs were based on city-block distance. The distance was computed from average miRNA expressions in normal, grade I, grade II and grade III groups, respectively.

### Soft agar assays and 3D cell culture

Soft agar assays were performed as previously described.<sup>21</sup> For 3D cell culture, MCF-10A cells were dissociated into single cells and cultured with Dulbecco's modified Eagle medium/F-12 containing 5% Matrigel, 5% heat-inactivated FBS, 0.5  $\mu$ g/ml hydrocortisone, 100 ng/ml cholera toxin, 10  $\mu$ g/ml insulin, 10 ng/ml EGF and 5  $\mu$ M Y-27632. Cells were embedded into Matrigel-coated chamber slides and grown for 7–14 days, with replacement of fresh assay medium every 4 days. Fluorescence was visualized using an Olympus IX81

spinning disk confocal microscope (Olympus, Tokyo, Japan). The images presented are representative of three independent experiments.

### Human tissue arrays and locked nucleic acid-based *in situ* hybridization

Paraffin sections containing 43 breast tumor samples and 5 normal breast tissue samples (BR480, US Biomax, Rockville, MD, USA) were incubated with miR-140 probe to visualize miR-140 expression in tissues. *In situ* hybridization for miR-140 has been published using 5'-digoxigenin-tagged probe.<sup>48</sup> Five-micrometer-thin sections of breast tissues adhered to glass slides were deparaffinized in three consecutive xylene baths for 5 min each, followed by 3 min each in serial dilutions of ethanol (100, 95, 80, 70 and 50%) and three changes of diethyl pyrocarbonate (DEPC)-treated water. Slides were digested with 5 µg/ml proteinase K, incubated with 95% ethanol and air-dried. Slides were hybridized with locked nucleic acid-modified miR-140 probe and incubated with anti-5'-digoxigenin antibodies (1:200 in PBS + 10% FBS). Colorimetric detection reaction was performed using NBT/BCIP Ready Mix (Roche) for 3 days. The slides were stained with Nuclear Fast Red (Sigma) and mounted in Prolong Gold. The nucleic acid-based *in situ* hybridization results were scored based on the percentage of positive cells.

### Xenograft studies

Animal studies complied with federal guidelines and institutional policies by the University of Maryland Animal Care and Use Committee. Immunodeficient nude female mice were purchased from Charles River Laboratories (Wilmington, MA, USA). Mice aged 5–6 weeks were randomized into two groups, with total number of mice in each group being five. DCIS cells (whole cells or mammosphere cells) stably expressing nontargeted control and miR-140-overexpressing cells were washed twice with cold PBS and trypsinized. Immediately before injection, cells (whole cells, mammosphere cells or CD44 high/CD24 low stem cells) were resuspended with 100 µl of media/Matrigel (1:1). The cells were injected near each no. 5 mammary gland nipple. Tumor growth was monitored weekly by digital caliper measurements (tumor size = (length × width<sup>2</sup>)/2). At the end of the experiment, tumors were fixed in formalin.

### Statistical analysis

Statistical analysis was performed by Student's *t*-test. *P*-values of <0.05 (\*) were considered significant. Data are presented as mean±s.e.m. Data were analyzed using GraphPad Prism 4.0 (Graphpad Software, San Diego, CA, USA).

### Supplementary Material

Refer to Web version on PubMed Central for supplementary material.

### Acknowledgments

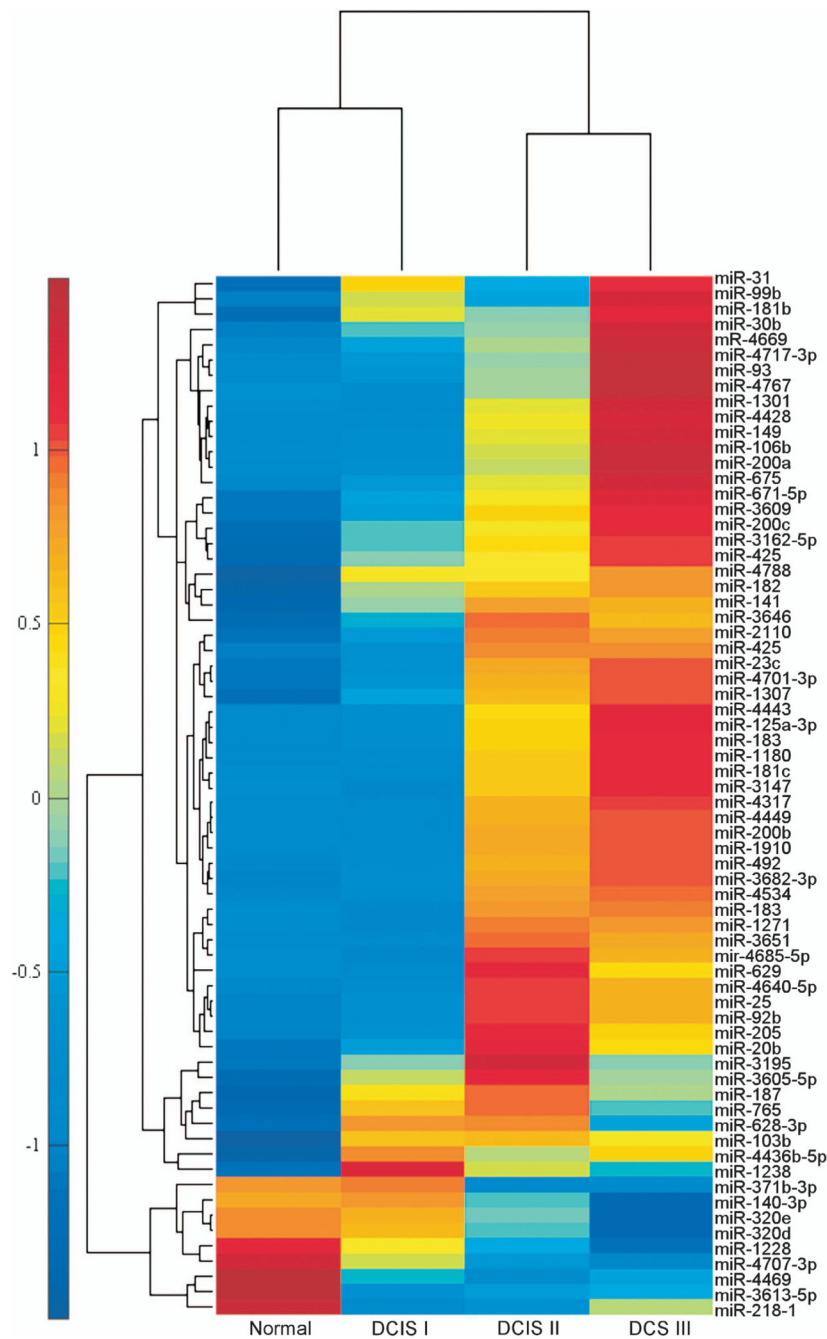
This work was supported by grants from Maryland Stem Cell Fund, FAMRI, ACS and NCI R01 (QZ), and NCI T32 training (GE).

## References

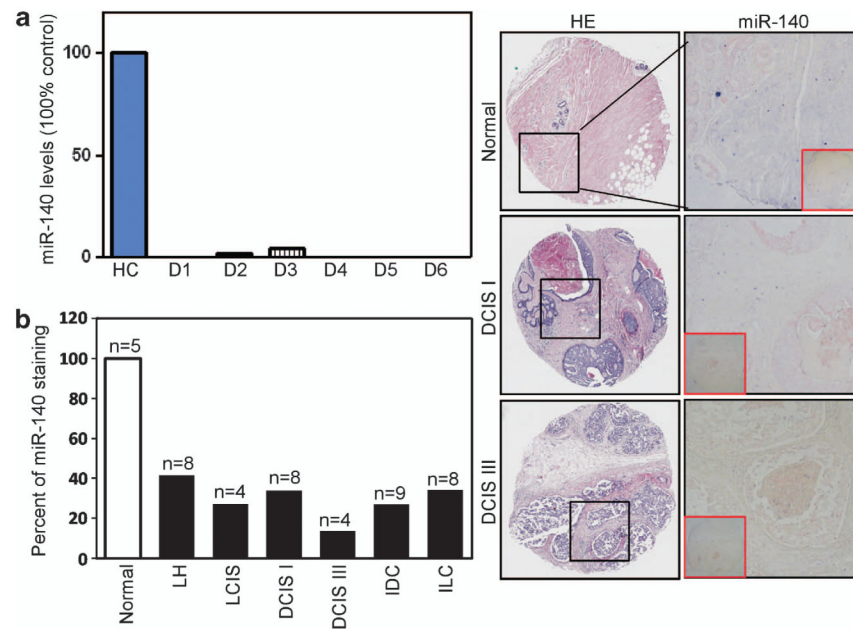
1. Leonard GD, Swain SM. Ductal carcinoma *in situ*, complexities and challenges. *J Natl Cancer Inst.* 2004; 96:906–920. [PubMed: 15199110]
2. Jemal A, Siegel R, Ward E, Murray T, Xu J, Thun MJ. Cancer statistics, 2007. *Cancer J Clin.* 2007; 57:43–66.
3. Li CI, Daling JR, Malone KE. Age-specific incidence rates of *in situ* breast carcinomas by histologic type, 1980 to 2001. *Cancer Epidemiol Biomarkers Prev.* 2005; 14:1008–1011. [PubMed: 15824180]
4. Ernster VL, Ballard-Barbash R, Barlow WE, Zheng Y, Weaver DL, Cutter G, et al. Detection of ductal carcinoma *in situ* in women undergoing screening mammography. *J Natl Cancer Inst.* 2002; 94:1546–1555. [PubMed: 12381707]
5. Poller DN, Barth A, Slamon DJ, Silverstein MJ, Gierson ED, Coburn WJ, et al. Prognostic classification of breast ductal carcinoma-*in-situ*. *Lancet.* 1995; 345:1154–1157. [PubMed: 7723550]
6. Solin LJ, Yeh I, Kurtz J, Fourquet A, Recht A, Kurske R, et al. Ductal carcinoma *in situ* (intraductal carcinoma) of the breast treated with breast-conserving surgery and definitive irradiation correlation of pathologic parameters with outcome of treatment. *Cancer.* 1993; 71:2532–2542. [PubMed: 8384070]
7. Fisher B, Dignam J, Wolmark N, Mamounas E, Costantino J, Poller W, et al. Lumpectomy and radiation therapy for the treatment of intraductal breast cancer: findings from National Surgical Adjuvant Breast and Bowel Project B-17. *J Clin Oncol.* 1998; 16:441–452. [PubMed: 9469327]
8. Fowble B, Hanlon A, Fein D, Hoffman J, Sigurdson E, Patchefsky A, et al. Results of conservative surgery and radiation for mammographically detected ductal carcinoma *in situ* (DCIS). *Int J Radiat Oncol Biol Phys.* 1997; 38:949–957. [PubMed: 9276359]
9. Lenington WJ, Jensen RA, Dalton LW, Page DL. Ductal carcinoma *in situ* of the breast. Heterogeneity of individual lesions. *Cancer.* 1994; 73:118–124. [PubMed: 8275415]
10. Fisher B, Land S, Mamounas E, Dignam J, Fisher ER, Wolmark N. Prevention of invasive breast cancer in women with ductal carcinoma *in situ*: an update of the National Surgical Adjuvant Breast and Bowel Project experience. *Semin Oncol.* 2001; 28:400–418. [PubMed: 11498833]
11. Houghton J. Radiotherapy and tamoxifen in women with completely excised ductal carcinoma *in situ* of the breast in the UK, Australia, and New Zealand: randomized controlled trial. *Lancet.* 2003; 362:95–102. [PubMed: 12867108]
12. Espina V, Mariani BD, Gallagher RI, Tran K, Banks S, Wiedemann J, et al. Malignant precursor cells pre-exist in human breast DCIS and require autophagy for survival. *PLoS One.* 2010; 5:e10240. [PubMed: 20421921]
13. Visvader JE, Lindeman GJ. Cancer stem cells in solid tumours: accumulating evidence and unresolved questions. *Nat Rev Cancer.* 2008; 8:755–768. [PubMed: 18784658]
14. Takebe N, Ivy SP. Controversies in cancer stem cells: targeting embryonic signaling pathways. *Clin Cancer Res.* 2010; 16:3106–3112. [PubMed: 20530695]
15. Farnie G, Clarke R. Mammary stem cells and breast cancer--role of Notch signalling. *Stem Cell Rev.* 2007; 3:169–175. [PubMed: 17873349]
16. Calin GA, Croce CM. MicroRNA signatures in human cancers. *Nat Rev Cancer.* 2006; 6:857–866. [PubMed: 17060945]
17. Ruan K, Fang X, Ouyang G. MicroRNAs: novel regulators in the hallmarks of human cancer. *Cancer Lett.* 2009; 285:116–126. [PubMed: 19464788]
18. Vrba L, Garbe JC, Stampfer MR, Futscher BW. Epigenetic regulation of normal human mammary cell type-specific miRNAs. *Genome Res.* 2011; 21:2026–2037. [PubMed: 21873453]
19. Farazi TA, Horlings HM, ten Hoeve JJ, Mihailovic A, Halfwerk H, Morozov P, et al. MicroRNA sequence and expression analysis in breast tumors by deep sequencing. *Cancer Res.* 2011; 71:4443–4453. [PubMed: 21586611]
20. Volinia S, Galasso M, Sana ME, Wise TF, Palantini J, Huebner K, et al. Breast cancer signatures for invasiveness and prognosis defined by deep sequencing of microRNA. *Proc Natl Acad Sci USA.* 2012; 109:3024–3029. [PubMed: 22315424]

21. Eades G, Yao Y, Yang M, Zhang Y, Chumsri S, Zhou Q. miR-200a regulates SIRT1 expression and epithelial to mesenchymal transition (EMT)-like transformation in mammary epithelial cells. *J Biol Chem*. 2011; 286:25992–26002. [PubMed: 21596753]
22. Lehmann U, Hasemeier B, Christgen M, Muller M, Romermann D, Langer F, et al. Epigenetic inactivation of microRNA gene hsa-mir-9-1 in human breast cancer. *J Pathol*. 2008; 214:17–24. [PubMed: 17948228]
23. de Souza RS, Breiling A, Gupta N, Malekpour M, Youns M, Omranipour R, et al. Epigenetically deregulated microRNA-375 is involved in a positive feedback loop with estrogen receptor  $\alpha$  in breast cancer cells. *Cancer Res*. 2010; 70:9175–9184. [PubMed: 20978187]
24. Yang J, Qin S, Yi C, Ma G, Zhu G, Zhou W, et al. MiR-140 is co-expressed with Wwp2-C transcript and activated by Sox9 to target Sp1 in maintaining the chondrocyte proliferation. *FEBS Lett*. 2011; 585:2992–2997. [PubMed: 21872590]
25. Takai D, Jones PA. The CpG island searcher: a new WWW resource. *In Silico Biol*. 2003; 3:235–240. [PubMed: 12954087]
26. Livasy CA, Perou CM, Karaca G, Cowan DW, Maia D, Jackson S, et al. Identification of a basal-like subtype of breast ductal carcinoma *in situ*. *Hum Pathol*. 2007; 38:197–204. [PubMed: 17234468]
27. Zhou W, Jirstrom K, Johansson C, Amini R, Blomqvist C, Agbaje O, et al. Long-term survival of women with basal-like ductal carcinoma *in situ* of the breast: a population-based cohort study. *BMC Cancer*. 2010; 10:653. [PubMed: 21118480]
28. Miller FR, Santner SJ, Tait L, Dawson PJ. MCF10DCIS.com Xenograft model of human comedo ductal carcinoma *in situ*. *J Natl Cancer Inst*. 2000; 92:1185a–1186a. [PubMed: 10904098]
29. Tait LR, Pauley RJ, Santner SJ, Heppner GH, Heng HH, Rak JW, et al. Dynamic stromal-epithelial interactions during progression of MCF10DCIS.com xenografts. *Int J Cancer*. 2007; 120:2127–2134. [PubMed: 17266026]
30. Scribner KC, Behbod F, Porter WW. Regulation of DCIS to invasive breast cancer progression by Single-minded-2s (SIM2s). *Oncogene*. 2012; 32:2631–2639. [PubMed: 22777354]
31. Myzak MC, Hardin K, Wang R, Dashwood RH, Ho E. Sulforaphane inhibits histone deacetylase activity in BPH-1, LnCaP and PC-3 prostate epithelial cells. *Carcinogenesis*. 2006; 27:811–819. [PubMed: 16280330]
32. Hsu A, Wong C, Yu Z, Williams D, Dashwood R, Ho E. Promoter demethylation of cyclin D2 by sulforaphane in prostate cancer cells. *Clin Epigenetics*. 2011; 3:3. [PubMed: 22303414]
33. Shackleton M, Vaillant F, Simpson KJ, Stingl J, Smyth GK, Asselin-Labat M, et al. Generation of a functional mammary gland from a single stem cell. *Nature*. 2006; 439:84–88. [PubMed: 16397499]
34. Stingl J, Eirew P, Ricketson I, Shackleton M, Vaillant F, Choi D, et al. Purification and unique properties of mammary epithelial stem cells. *Nature*. 2006; 439:993–997. [PubMed: 16395311]
35. Al-Hajj M, Wicha MS, Benito-Hernandez A, Morrison SJ, Clarke MF. Prospective identification of tumorigenic breast cancer cells. *Proc Natl Acad Sci USA*. 2003; 100:3983–3988. [PubMed: 12629218]
36. Liu S, Clouthier S, Wicha M. Role of microRNAs in the regulation of breast cancer stem cells. *J Mammary Gland Biol Neoplasia*. 2012; 17:15–21. [PubMed: 22331423]
37. Ricardo S, Vieira AF, Gerhard R, Leitao D, Pinto R, Cameselle-Teijeiro J, et al. Breast cancer stem cell markers CD44, CD24 and ALDH1: expression distribution within intrinsic molecular subtype. *J Clin Pathol*. 2011; 64:937–946. [PubMed: 21680574]
38. de Beça FF, Caetano P, Gerhard R, Alvarenga CA, Gomes M, Paraedes J, et al. Cancer stem cells markers CD44, CD24 and ALDH1 in breast cancer special histological types. *J Clin Pathol*. 2013; 66:187–191. [PubMed: 23112116]
39. Guo W, Keckesova Z, Donaher J, Shibue T, Tischler V, Reinhardt F, et al. Slug and Sox9 cooperatively determine the mammary stem cell state. *Cell*. 2012; 148:1015–1028. [PubMed: 22385965]
40. Ginestier C, Hur MH, Charafe-Jaufret E, Monville F, Dutcher J, Brown M, et al. ALDH1 is a marker of normal and malignant human mammary stem cells and a predictor of poor clinical outcome. *Cell Stem Cell*. 2007; 1:555–567. [PubMed: 18371393]

41. Kao J, Salari K, Bocanegra M, Choi Y, Girard L, Gandhi J, et al. Molecular profiling of breast cancer cell lines defines relevant tumor models and provides a resource for cancer gene discovery. *PLoS One*. 2009; 4:e6146. [PubMed: 19582160]
42. Dontu G, Abdallah WM, Foley JM, Jackson KW, Clarke MF, Kawamura MJ, et al. *In vitro* propagation and transcriptional profiling of human mammary stem/progenitor cells. *Genes Dev*. 2003; 17:1253–1270. [PubMed: 12756227]
43. Tsai H, Li H, Van Neste L, Cai Y, Robert C, Rassool F, et al. Transient low doses of dna-demethylating agents exert durable antitumor effects on hematological and epithelial tumor cells. *Cancer Cell*. 2012; 21:430–446. [PubMed: 22439938]
44. Shimono Y, Zabala M, Cho RW, Lobo N, Dalerba P, Qian D, et al. Downregulation of miRNA-200c links breast cancer stem cells with normal stem cells. *Cell*. 2009; 138:592–603. [PubMed: 19665978]
45. Johnson SM, Grosshans H, Shingara J, Byrom M, Jarvis R, Cheng A, et al. RAS is regulated by the let-7 microRNA family. *Cell*. 2005; 120:635–647. [PubMed: 15766527]
46. Kong D, Heath E, Chen W, Cher ML, Powell I, Heilbrun L, et al. Loss of Let-7 up-regulates EZH2 in prostate cancer consistent with the acquisition of cancer stem cell signatures that are attenuated by BR-DIM. *PLoS One*. 2012; 7:e33729. [PubMed: 22442719]
47. Kumarswamy R, Mudduluru G, Ceppi P, Muppala S, Kozlowski M, Niklinski J, et al. MicroRNA-30a inhibits epithelial-to-mesenchymal transition by targeting Snai1 and is downregulated in non-small cell lung cancer. *Int J Cancer*. 2012; 130:2044–2053. [PubMed: 21633953]
48. Yamashita S, Miyaki S, Kato Y, Yokoyama S, Sato T, Barrionuevo F, et al. L-Sox5 and Sox6 enhance chondrogenic miR-140 expression by strengthening dimeric Sox9 activity. *J Biol Chem*. 2012; 287:22206–22215. [PubMed: 22547066]



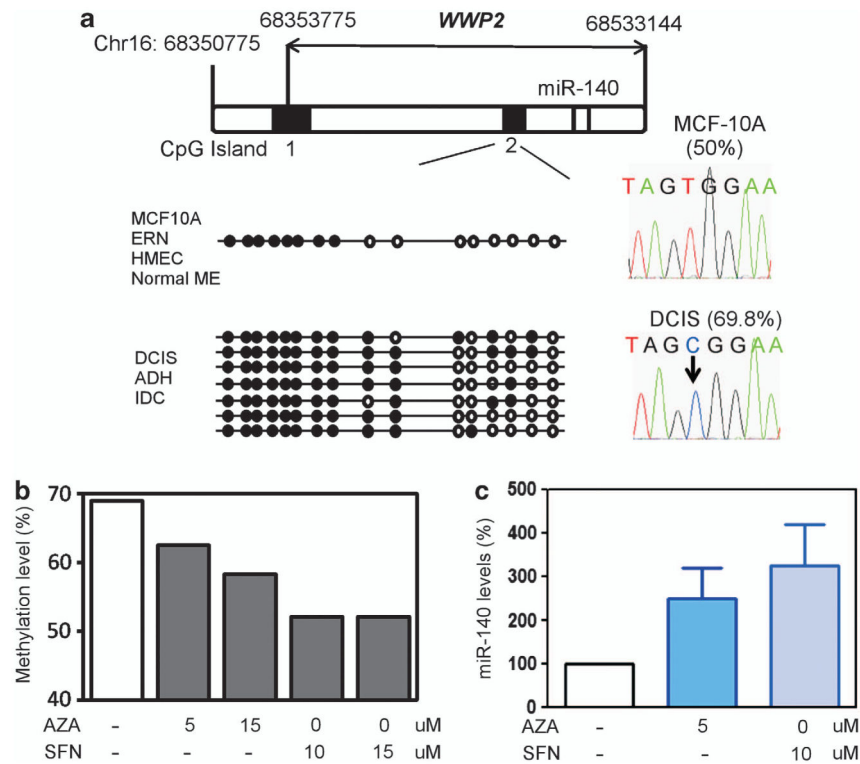
**Figure 1.** miRNA profiling from DCIS lesions and matched normal breast tissues. (a) Genome-wide microarray analysis of miRNA expression in DCIS (low grade (I), intermediate grade (II), high grade (III),  $n = 6$ ) and matched normal control tissues. Hybridizations and measurements were performed, and 68 miRs are shown that demonstrated more than two-fold change, with  $P < 0.05$  between average DCIS and matched normal samples. Heatmap showing hierarchical clusters of miRNAs and distance from average expression in normal, grade I, grade II and grade III DCIS lesions.



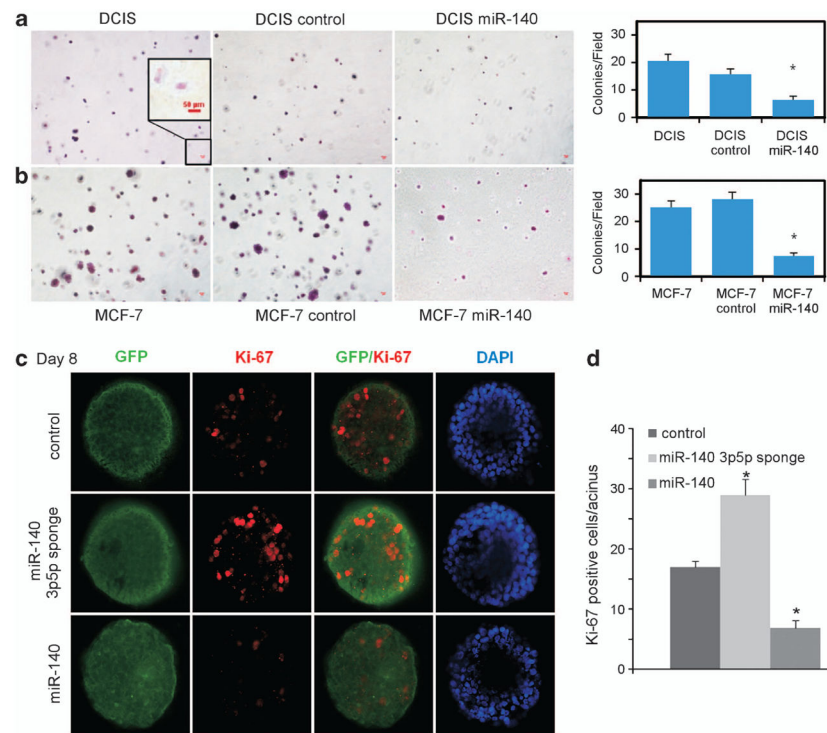
**Figure 2.**

Downregulation of miR-140 in breast tumor tissues. **(a)** qRT-PCR analysis of miR-140 expression in normal breast tissue and fresh tumor tissue from patients with DCIS ( $n = 22$ , results from six basal-like lesions), normalizing to U6 small nuclear (snRNA). **(b)** Validation of miR-140 downregulation in different breast cancer tissues. *In situ* hybridization of miR-140 probe (5'-digoxigenin, DIG-tagged) in 43 breast tumor samples and five normal human breast tissue samples (BR480 Breast Tissue Array, US Biomax). Staining with anti-DIG antibodies was visualized through colorimetric NBT/BCIP reaction (blue staining). Quantification is shown as percentage of positively staining cells. LH = atypical lobular hyperplasia, LCIS = lobular carcinoma *in situ*, DCIS I = ductal carcinoma *in situ* nuclear grade I, DCIS III = comedo ductal carcinoma *in situ* (grade III), IDC = invasive ductal carcinoma, ILC = invasive lobular carcinoma.

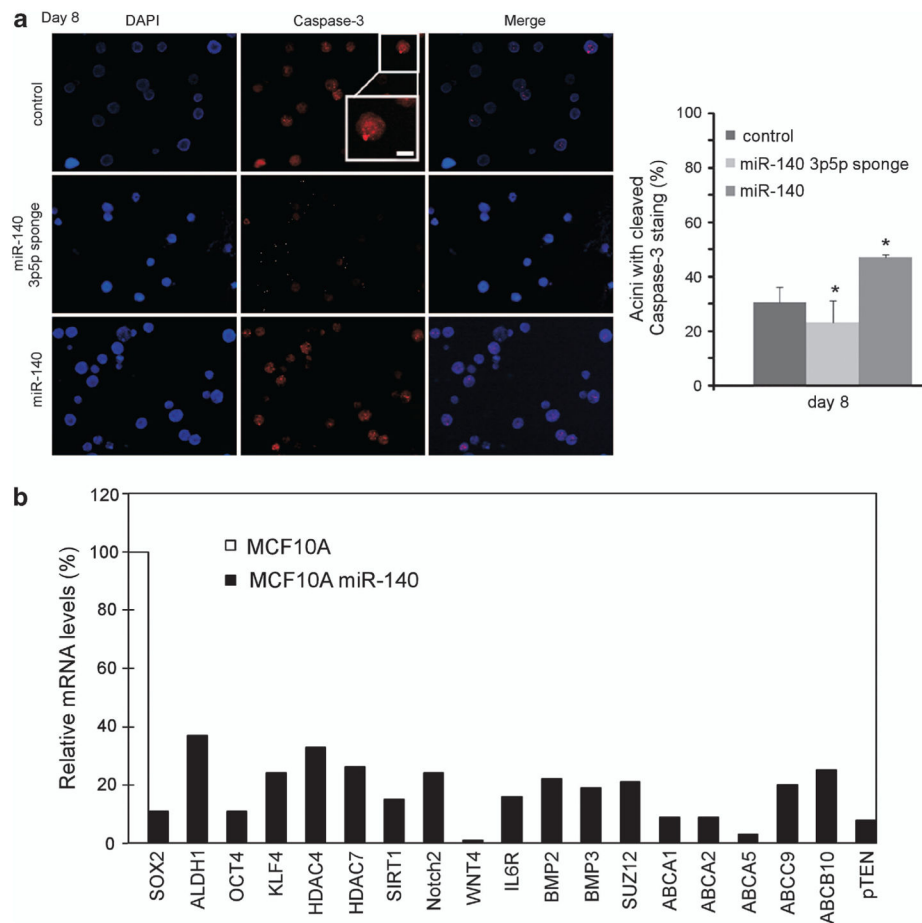


**Figure 3.**

Epigenetic dysregulation of miR-140 in DCIS lesions. **(a)** Identification of two CpG islands within the *WWP2* locus (chromosome 16: 68350775–68533144). Bisulfite sequencing of CpG islands was performed on normal tissue/cell lines and breast tumor tissue/cell lines. Differential methylation of CpG island 2 is shown in diagram. % methylation is shown for parental MCF-10A cells and MCF10DCIS cells. **(b)** Treatment with epigenetic therapy (5-Aza-2'-deoxycytidine (AZA) and sulforaphane (SFN)) restores normal-like methylation levels. **(c)** Treatment with epigenetic therapy (AZA or SFN) restores miR-140 expression, as determined by qRT-PCR, normalizing to U6 snRNA levels.  $n = 3 \pm s.e.$

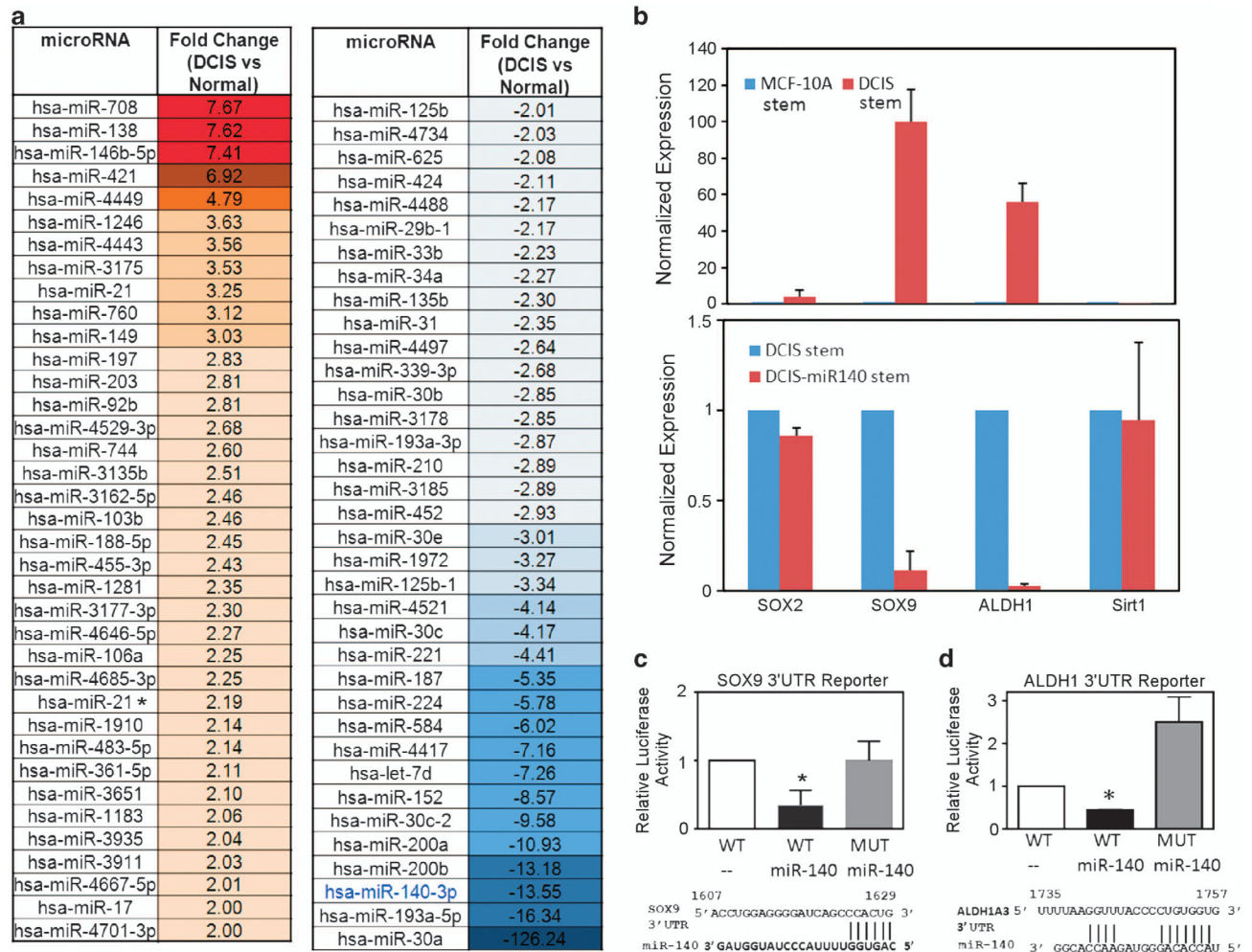


**Figure 4.** miR-140 is a tumor suppressor in a model of basal-like DCIS. **(a)** miR-140 overexpression results in decreased anchorage-independent growth in soft agar. MCF10DCIS cells were transfected with miR-140 expression vector or control vector and were grown in agarose (0.3%) for 3 weeks. Colonies were stained with crystal violet and visualized, and counted by light microscopy.  $n = 3 \pm s.e.$  **(b)** MCF-7 (positive control for ‘transformed’ cells) were transfected with miR-140 expression vector or control vector and were grown in agarose for 3 weeks, stained with crystal violet and quantified by light microscopy. **(c)** 3-D cell culture of MCF-10A cells transfected with miR-140 expression vector, miR-140-3p/5p ‘sponge’ inhibitor or control vectors. Cells were stained with anti-Ki67 antibody and anti-rabbit Alexa 488 or 555-conjugated secondary antibody. Nuclei were DAPI (4’,6-diamidino-2-phenylindole)-counterstained. **(d)** Quantification of percent Ki67-positive cells from three independent experiments (\* $P < 0.01$ ).



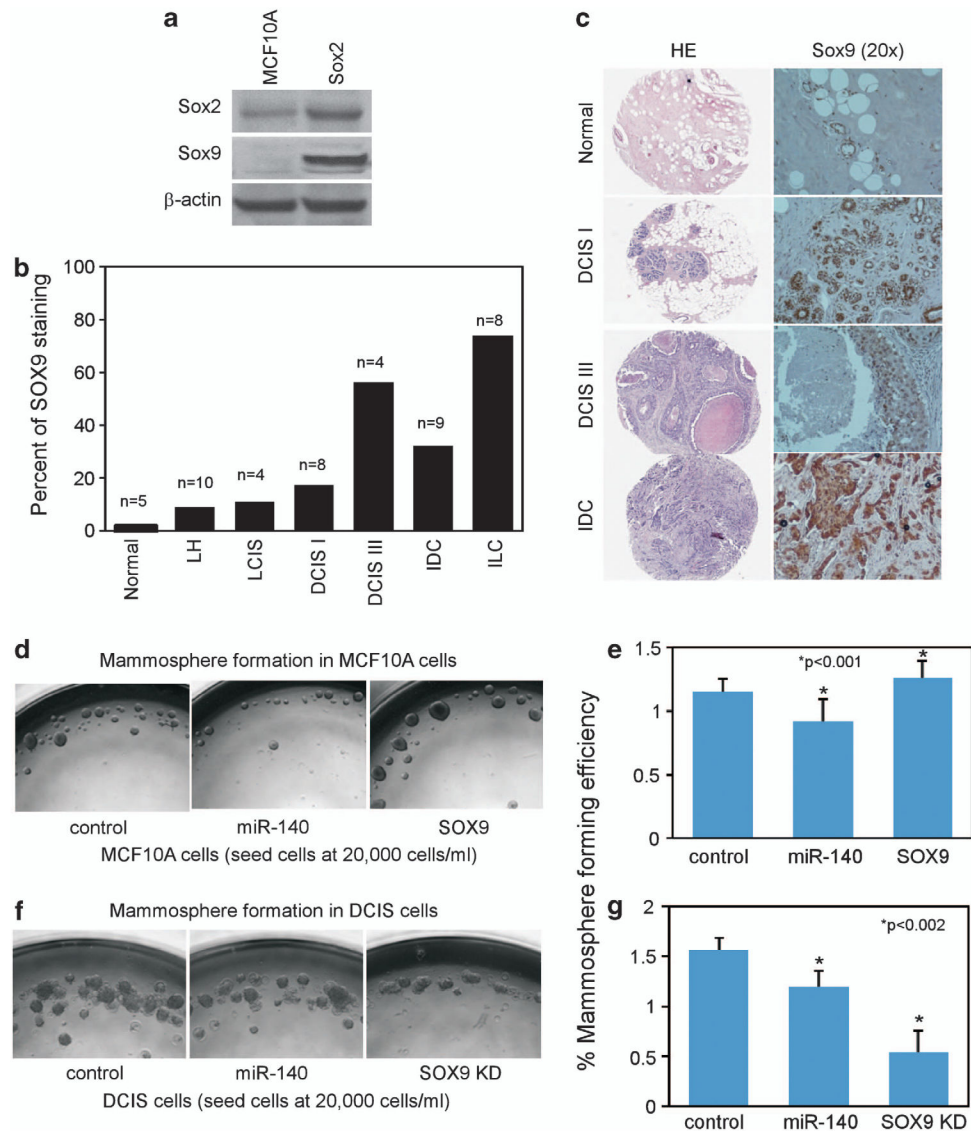
**Figure 5.**

The tumor suppressor miR-140 regulates numerous stem-cell factors in mammary epithelial cells. **(a)** 3-D cell culture of MCF-10A cells transfected with miR-140 expression vector, miR-140-3p/5p ‘sponge’ inhibitor or control vectors. Cells were stained with anti-caspase-3 (activated) antibody and anti-rabbit Alexa 488 or 555-conjugated secondary antibody. Nuclei were DAPI-counterstained. Quantification of percent caspase-3-positive cells from three independent experiments. **(b)** MCF10A cells were infected with lentiviral miR-140 vectors, and mRNA from pooled cells was analyzed by qRT-PCR. Numerous stem-cell factors that are predicted miR-140 targets were downregulated in stably miR-140-overexpressing MCF-10A cells compared with control cells (Student’s *t*-test, \* $P < 0.01$ ).



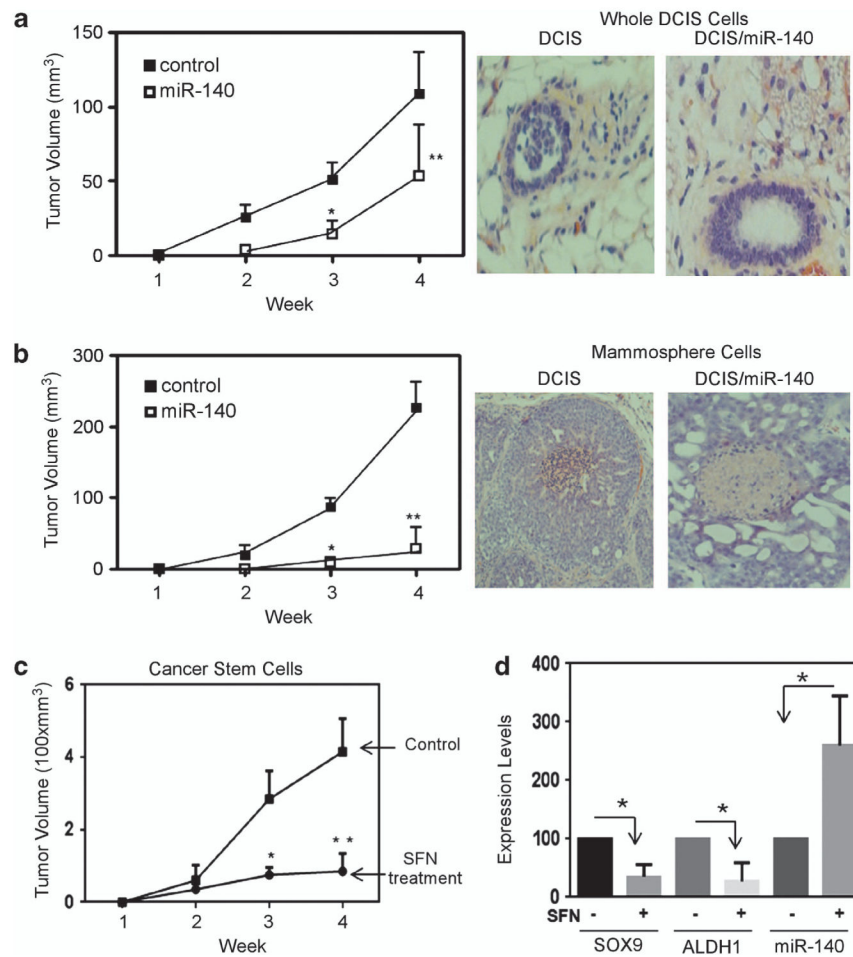
**Figure 6.** miR-140 downregulation correlates with SOX9 and ALDH1 activation in DCIS cancer stem-like cells. **(a)** Comparisons of mammary stem cells and DCIS cancer stem-like cells revealed dysregulation of 72 miRNAs in DCIS cancer stem-like cells. miR-140 was downregulated –13.55-fold in DCIS stem-like cells. Normal stem cells from parental MCF-10A cells (CD44 high/CD24 low) and cancer stem-like cells from MCF10DCIS (CD44 high/CD24 low) were isolated by fluorescent-activated cell sorting (FACS). miRNA profiling was performed on extracted RNA using GeneChip miRNA Array v3.0 (Affymetrix). miRNA\* indicates miRNA star sequence. **(b–d)** SOX9 and ALDH1 stem cell regulators are critical targets of miR-140 in DCIS stem cells **(b)**, (upper) SOX9 and ALDH1 are dramatically upregulated in DCIS stem-like cells compared with MCF-10A mammary stem cells. mRNA expression was compared using qRT–PCR normalizing to GAPDH. (lower) DCIS stem cells and DCIS stem cell overexpressing miR-140. Forced expression of miR-140 reduced SOX9 and ALDH1 expression in DCIS stem-like cells. **(c)** HEK-293T cells were transfected with pGL3 luciferase reporter containing wild-type SOX9-3'-UTR or mutant SOX9-3'-UTR (abolishing miR-140 response element) along with miR-140 expression vector. After 48 h, cells were lysed and luciferase activity was measured with a

luminometer. Predicted miR-140 targeting site in SOX9-3'-UTR is shown along with the bases, which were mutated in the seeding site. **(d)** HEK-293T cells were transfected with pGL3 luciferase reporter, containing wild-type ALDH1-3'-UTR or mutant ALDH1-3'-UTR (abolishing miR-140 response element) along with miR-140 expression vector. After 48 h, cells were lysed and luciferase activity was measured with a luminometer. Predicted miR-140 targeting site in ALDH1-3'-UTR is shown along with the bases, which were mutated in the seeding site.  $n = 3$ ,  $*P < 0.05$ .

**Figure 7.**

SOX9 is overexpressed in multiple breast cancer malignancies including DCIS. (a) Western blotting showing SOX9 upregulation in MCF10DCIS cells compared with parental MCF-10A cells. SOX2 is shown for comparison.  $\beta$ -actin was used as a loading control. (b) Quantification of SOX9 staining from breast tumor tissue array (BR480 Breast Tissue Array, US Biomax). FFPE human breast tumors and normal breast tissue samples were stained with rabbit anti-SOX9 antibodies. Brown precipitate was developed using avidin-biotin peroxidase substrate kit (Vector Laboratories, Burlingame, CA, USA). Nuclei were counterstained with hematoxylin. Quantitative analysis was done to determine percentage of positively nuclear stained mammary epithelial cells. LH = atypical lobular hyperplasia, LCIS = lobular carcinoma *in situ*, DCIS I = ductal carcinoma *in situ* nuclear grade 1, DCIS III = comedo ductal carcinoma *in situ* (grade III), IDC = invasive ductal carcinoma, ILC = invasive lobular carcinoma. (c) Representative SOX9 staining of DCIS grade I, DCIS grade III and IDC. SOX9 is visualized via brown precipitate. (d, e) MCF-10A cells were

transfected with miR-140 overexpression vector or SOX9 overexpression vector. Transfected MCF-10A cells were collected via nonenzymatic dissociation buffer, separated with 40- $\mu$ m cell strainers and were seeded at 20 000 cells/ml on attachment-free six-well plates. Mammospheres were analyzed and photographed after 7 days and mammospheres >100  $\mu$ m in size were quantified. **(f, g)** DCIS.COM cells were transfected with miR-140 overexpression vector or SOX9 shRNA vector. Transfected MCF10DCIS cells were collected via nonenzymatic dissociation buffer, separated with 40- $\mu$ m cell strainers and were seeded at 20 000 cells/ml on attachment-free six-well plates. Mammospheres were analyzed and photographed after 7 days and mammospheres >100  $\mu$ m in size were quantified.  $n = 3 \pm$ s.e. for **e** \* $P < 0.001$ , for **g** \* $P < 0.002$ .

**Figure 8.**

Activation of miR-140 reduces stem cell renewal and tumor growth *in vivo*. **(a)**  $10^6$  stable (lentiviral) miR-140-overexpressing ( $n = 5$ ) or nontargeted control overexpressing ( $n = 5$ ) MCF10DCIS cells (whole-cell populations) were injected into the mammary gland of nude mice. Tumor growth was analyzed weekly using digital calipers to calculate tumor volume ( $\text{mm}^3$ ). (Right) photographs of mammary ducts and DCIS lesions. **(b)** A total of 10 000 mammosphere cells stably overexpressing miR-140 ( $n = 5$ ) or control ( $n = 5$ ) were injected into mammary gland of nude mice. Tumor volume was analyzed weekly using digital calipers. (Right) photographs of mammary ducts and DCIS lesions. **(c)** FACS-isolated CD44 high/CD24 low DCIS stem-like cells ( $n = 8$ ) and sulforaphane-pretreated DCIS stem-like cells were injected into mammary glands. Tumor volume measured weekly is shown. **(d)** RNA was extracted from isolated tumor tissue and analyzed by qRT-PCR, normalizing to GAPDH (for SOX9 and ALDH1) or U6 snRNA (for miR-140) for **a,b,c** \* $P < 0.01$ , \*\* $P < 0.05$ , **d** \* $P < 0.05$ .